
# *Geochronology and geochemical analysis of Quaternary travertine deposits at the Belen quarries of Mesa Aparejo, NM: Evaluation of travertine facies for paleohydrology and paleoenvironment Studies*

Alexandra Priewisch, Laura J. Crossey, Karl E. Karlstrom, Hank S. Chafetz, and M.A. Cook
2016, pp. 405-418. https://doi.org/10.56577/FFC-67.405
Supplemental data: https://nmgs.nmt.edu/repository/index.cfml?rid=2016004

*in:*

*Guidebook 67 - Geology of the Belen Area*, Frey, Bonnie A.; Karlstrom, Karl E. ; Lucas, Spencer G.; Williams, Shannon; Zeigler, Kate; McLemore, Virginia; Ulmer-Scholle, Dana S., New Mexico Geological Society 67th Annual Fall Field Conference Guidebook, 512 p. https://doi.org/10.56577/FFC-67

*This page is intentionally left blank to maintain order of facing pages.*

New Mexico Geological Society Guidebook, 67th Field Conference, Geology of the Belen Area, 2016, p. 405-418.



# GEOCHRONOLOGY AND GEOCHEMICAL ANALYSIS OF QUATERNARY TRAVERTINE DEPOSITS AT THE BELEN QUARRIES OF MESA APAREJO, NM: EVALUATION OF TRAVERTINE FACIES FOR PALEOHYDROLOGY AND PALEOENVIRONMENT STUDIES

Alexandra Priewisch[1], Laura J. Crossey[1], Karl E. Karlstrom[1], Hank S. Chafetz[2], and M.A. Cook[2]

[1]Department of Earth and Planetary Sciences, University of New Mexico, Albuquerque, NM, alexandra.priewisch@gmail.com;
[2]Department of Geosciences, University of Houston, TX

**Abstract**—The depositional facies and stable isotopic composition of a large-volume Quaternary travertine deposit located in the Rio Grande rift in New Mexico provide a record of the paleohydrology of springs along the western Rio Grande rift flank. Our results show that lateral and vertical facies variations within a travertine deposit developed due to changing depositional environments, which are primarily related to the formation of travertine mounds sourced by springs along the rift-bounding Comanche and Santa Fe faults. Important travertine facies are 1) a terraced mound and sloping fan facies that represents surface flow, and 2) a vein facies that reflects artesian waters within the developing mounds. Stable oxygen and carbon isotope analyses of the two facies show similar $\delta^{18}O$ and $\delta^{13}C$ values, ranging between -6.6‰ and -9.3‰, and +1.3‰ and +6.1‰, respectively. The range of $\delta^{18}O$ values is similar to nearby springs along the west side of the rift and is interpreted to reflect variable mixing of endogenic (deeply derived) spring discharge with meteoric water. The $\delta^{13}C$ values are significantly higher than values of nearby springs ($\delta^{13}C$ = -1 to -8) and are interpreted to be controlled by variable $CO_2$ degassing rates. The age and volume of the travertine deposit suggests that the mounds archive an estimated minimum of 54 Gigatons $CO_2$ that degassed over a period of 456 ka along the fault system. Significant additional amounts of $CO_2$ likely escaped to the atmosphere during travertine formation and $\delta^{13}C$ fractionation. Travertine mound growth was facilitated by times of high $CO_2$ flux and times of high groundwater head in confined aquifer systems.

## INTRODUCTION

Travertines are groundwater discharge deposits that occur at many localities in the United States (Feth and Barnes, 1979; Ford and Pedley, 1996) and they provide useful paleoenvironmental data. Composed dominantly of the mineral calcite, travertines are datable with the U-series method, and their isotopic compositions may provide a geochemical record that can be used to model paleohydrology and paleoclimate (Minissale et al., 2002a; Smith et al., 2004; Andrews, 2006; Anzalone et al., 2007; Faccenna et al., 2008; Crossey et al., 2011; Kampman et al., 2012; Özkul et al., 2014). Stable oxygen isotopes of travertines can be used to evaluate the hydrologic conditions at the time of travertine deposition, i.e. water temperature and water composition, and terrestrial temperatures and precipitation patterns; whereas, stable carbon isotopes elucidate the origin of the $CO_2$ involved in travertine formation and $CO_2$ degassing rates (Chafetz and Lawrence, 1994; Andrews et al., 2000; Kele et al., 2008, 2011; Demeny et al., 2010; Özkul et al., 2014). Travertine formation is characterized by dynamic processes, which result in a variety of depositional environments, travertine morphologies and travertine facies (Chafetz and Folk, 1984; Pedley, 1990, 2009; Pentecost and Viles, 1994; Guo and Riding, 1998, 1999; Glover and Robertson, 2003; Pentecost, 2005; Jones and Renaut, 2010; Özkul et al., 2014; Barth and Chafetz, 2015).

In this study, we investigated a large-volume travertine deposit in New Mexico with the purpose of 1) providing a better understanding of lateral and vertical facies variations, 2) examining the impact of the depositional environment on the stable isotopic composition of travertine facies, and 3) estimating the amount of $CO_2$ and degassing rates that led to the formation of the large-volume travertine deposit.

## TRAVERTINE AND TRAVERTINE FORMATION

In this study, the term "travertine" is used for abiotically- and biotically-induced precipitated continental limestone that forms at springs and in streams (Ford and Pedley, 1996; Pentecost, 2005). The fresh-water carbonate deposits form due to the degassing of $CO_2$ from groundwater that is supersaturated with respect to calcium as well as biotically-induced carbonate precipitation according to the following reactions (Pentecost, 2005; Crossey et al., 2006, 2009):

$$CO_{2(g)} + H_2O + CaCO_{3(limestone)} \rightarrow Ca^{+}_{2\,(aq)} + 2HCO^{-}_{3\,(aq)}$$

$$Ca^{+}_{2\,(aq)} + 2HCO^{-}_{3\,(aq)} \rightarrow CO_{2(g)}\uparrow + H_2O + CaCO_{3(travertine)}$$

Travertine accumulations represent places of persistent and significant $CO_2$ degassing in spring systems that often occur along faults that can serve as conduits for deep-circulating waters and $CO_2$. The spring waters represent mixtures of hydro-

logic flow systems, including meteoric recharge, groundwater with long residence times, and deeply-derived fluids (Newell et al., 2005; Crossey et al., 2006, 2009; Embid, 2009; Williams et al., 2013). Several authors have suggested that travertine formation in the Southwestern United States occurred episodically on a 100 ka-scale at times when hydraulic head was high and when regional volcanic activity contributed excess magmatic/mantle-derived $CO_2$ to the system (e.g., Szabo, 1990, Embid, 2009, Cron, 2011, Crossey et al., 2011, Kampman et al., 2012, Tafoya, 2012, and Priewisch et al., 2014a).

## GEOLOGIC SETTING OF THE STUDY AREA

Travertine deposits in New Mexico are predominantly located along the Rio Grande rift and the Jemez lineament (Fig. 1). The Rio Grande rift consists of a series of north-south–trending sedimentary basins that extend over 1000 km from Colorado to Mexico and are bounded by extensional fault systems (e.g. Keller and Baldridge, 1999; Cather, 2004; Seager, 2004; Minor et al., 2013). The Jemez lineament is a prominent northeast–trending belt of Cenozoic volcanic fields that transect the southeastern Colorado Plateau (Aldrich, 1986; Dunbar, 2005; Chamberlin, 2007).

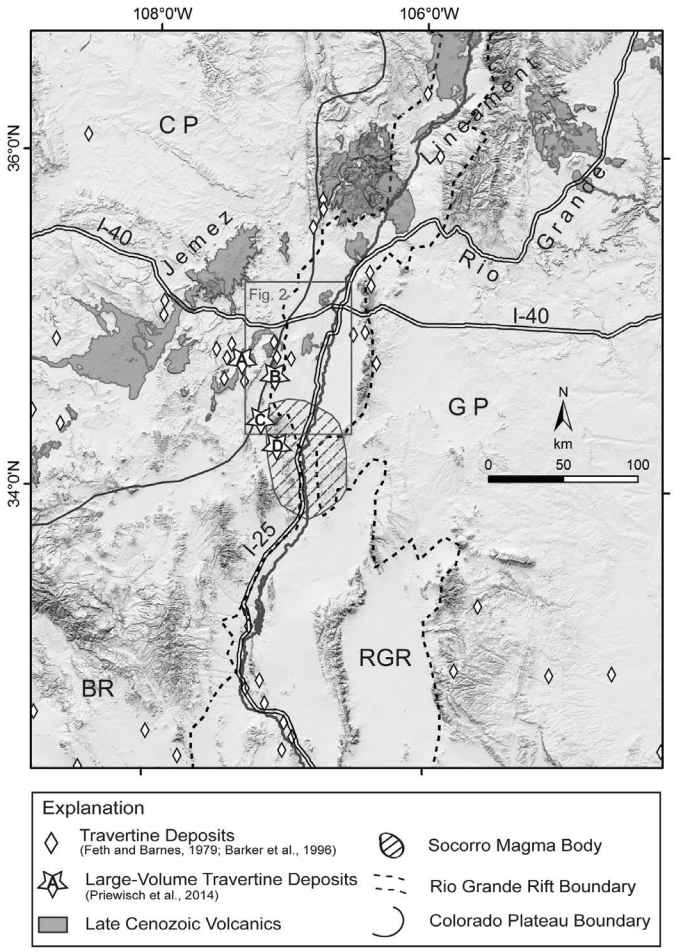


FIGURE 1. Locations of travertine accumulations (Feth and Barnes, 1979; Barker et al., 1996), large-volume travertine deposits (Priewisch et al., 2014a), the Rio Grande rift (RGR; black dashed line), and the Jemez lineament. Also shown are physiographic provinces: Colorado Plateau (CP), Great Plains (GP), and Basin and Range (BR). The large-volume travertine deposits are Mesa del Oro (A), Mesa Aparejo (B), Riley North Mesa (C), and Riley South Mesa (D). Grey box shows extent of Figure 2.

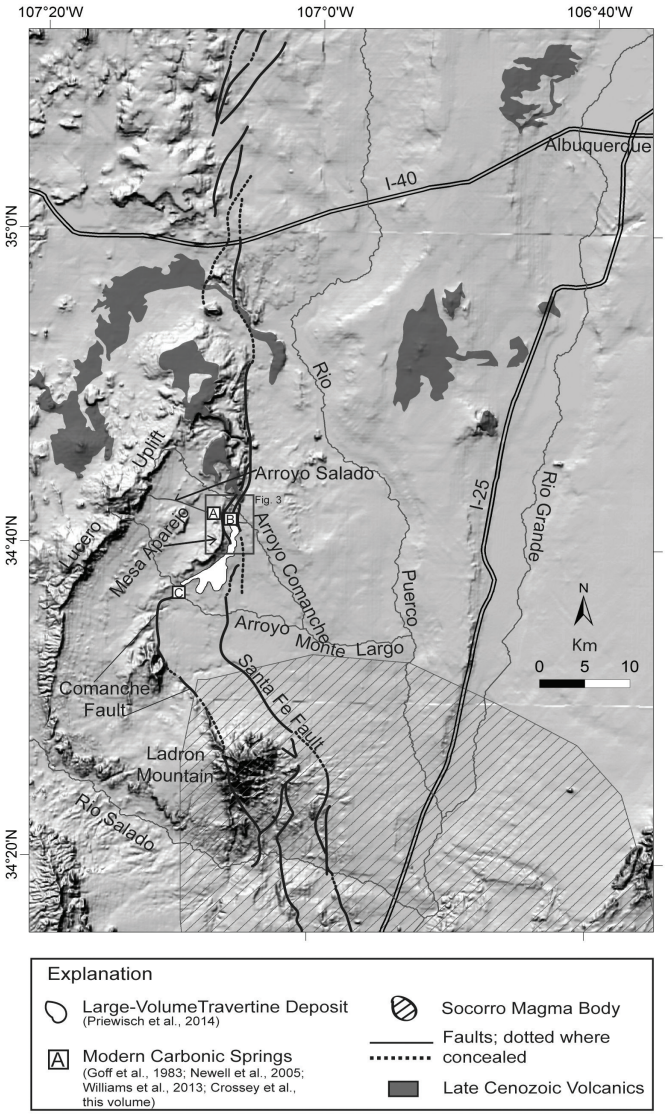


FIGURE 2. Map showing the large-volume travertine deposit at Mesa Aparejo (white area), the locations of active carbonic springs (Goff et al., 1983; Newell et al., 2005; Williams et al., 2013), and faults (New Mexico Bureau of Geology and Mineral Resources, 2003). The active springs are Arroyo Salado Spring (A), Red Hill Spring (B), and Four Daughters Springs (C). Grey box shows extent of Figure 3.

The large-volume travertine deposit of this study is located along the western edge of the Rio Grande rift, at Mesa Aparejo (Figs. 1, 2). Mesa Aparejo consists predominantly of Pennsylvanian limestone of the Madera Group (New Mexico Bureau of Geology and Mineral Resources, 2003) and is situated on the eastern side of the Lucero uplift along the Comanche fault (Fig. 2), a Laramide reverse fault that was modified during development of the Rio Grande rift (Callender and Zilinski, Jr, 1976; Ricketts et al., 2014). The travertine mounds are located between the Comanche and Santa Fe faults and the paleospring discharges appear to be concentrated along the Comanche fault

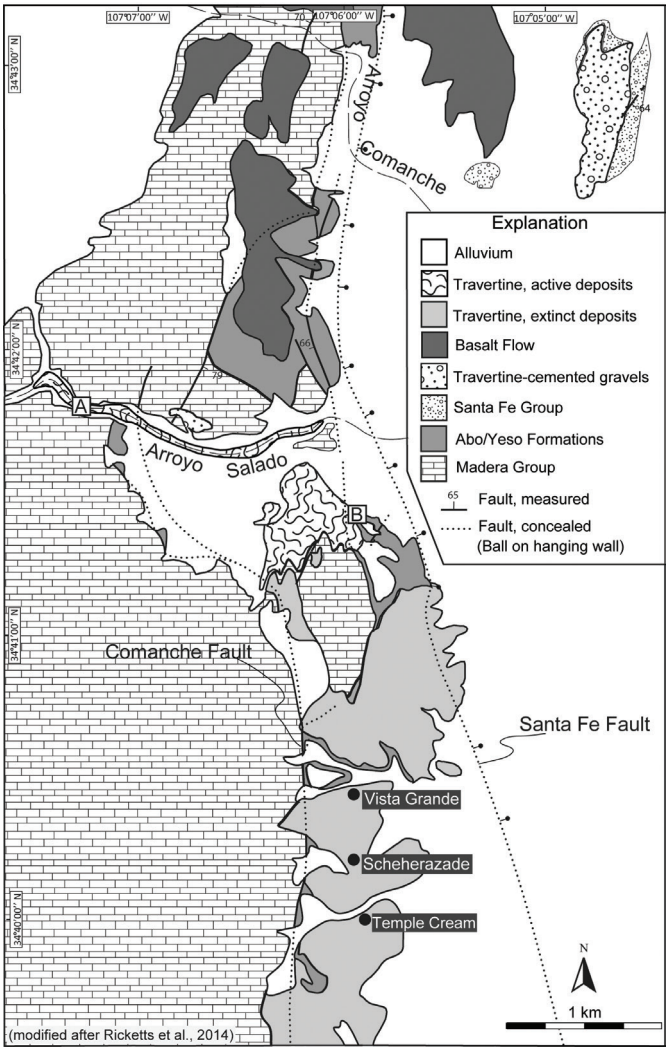


FIGURE 3. Map (modified after Ricketts et al., 2014) showing the northern part of the large-volume deposit at Mesa Aparejo, the surrounding geologic units, and location of the travertine quarries Temple Cream, Scheherazade, and Vista Grande. Also shown are the active travertine-depositing springs Arroyo Salado Spring (A) and Red Hill Spring (B).

(Figs. 2, 3). Mesa Aparejo is surrounded by Late Cenozoic basalt flows, which attest to significant volcanic activity in the area (Figs. 1, 2; Baldridge et al., 1987; Dunbar, 2005). Recent magmatic activity can be found south of Mesa Aparejo, in the central Rio Grande rift, where the Socorro magma body is located (Figs. 1, 2). The Socorro magma body is a sill-like intrusion at 19 km depth (Rinehart and Sanford, 1981; Ake and Sanford, 1988; Balch et al., 1997) that causes active uplift of the overlying region (Fialko and Simons, 2001; Pearse and Fialko, 2010; Reiter et al., 2010). According to heat flow data, the Socorro magma body represents the most recent manifestation of a much longer lived magmatic plumbing system (Reiter et al., 2010), which is thought to provide a source for mantle-derived $CO_2$ and $^3He$ (Newell et al., 2005; Williams et al., 2013). Modern carbonic springs located in arroyos close to the large-volume travertine deposits at Mesa Aparejo (Figs. 2, 3) attest to ongoing degassing of $CO_2$ and mantle-derived helium (Goff et al., 1983; Newell et al., 2005; Williams et al., 2013), but modern travertine precipitation at the springs and along the flow path of the water is significantly less than in the past.

The carbonic springs that discharged along the Comanche fault led to the formation of coalescing spring mounds that form the large-volume travertine deposits at Mesa Aparejo. These deposits cover an area of 13.1 $km^2$ and have a volume of ~0.2 $km^3$ (Priewisch et al., 2014a). At the time of writing, the northeastern part of the deposit is actively being quarried by New Mexico Travertine, Inc. (Austin and Barker, 1990), and the quarries provide exceptional outcrops of travertine facies, fabrics, and morphologies. The age of the quarried travertine ranges from more than 1.5 Ma to 254 ka (Priewisch et al., 2014a). This study focuses on three quarries in particular: Temple Cream, Scheherazade, and Vista Grande (Fig. 3; Austin and Barker, 1990).

Temple Cream is the southernmost and largest quarry (Fig. 3), with several quarry walls up to 9 m high (Fig. 4A). The color of the travertine is white to creamy-white. The quarry walls are cut by numerous open fractures ranging in width from a few millimeters to several tens of centimeters (Fig. 4A). Two travertine samples from the bottom and top of a measured section

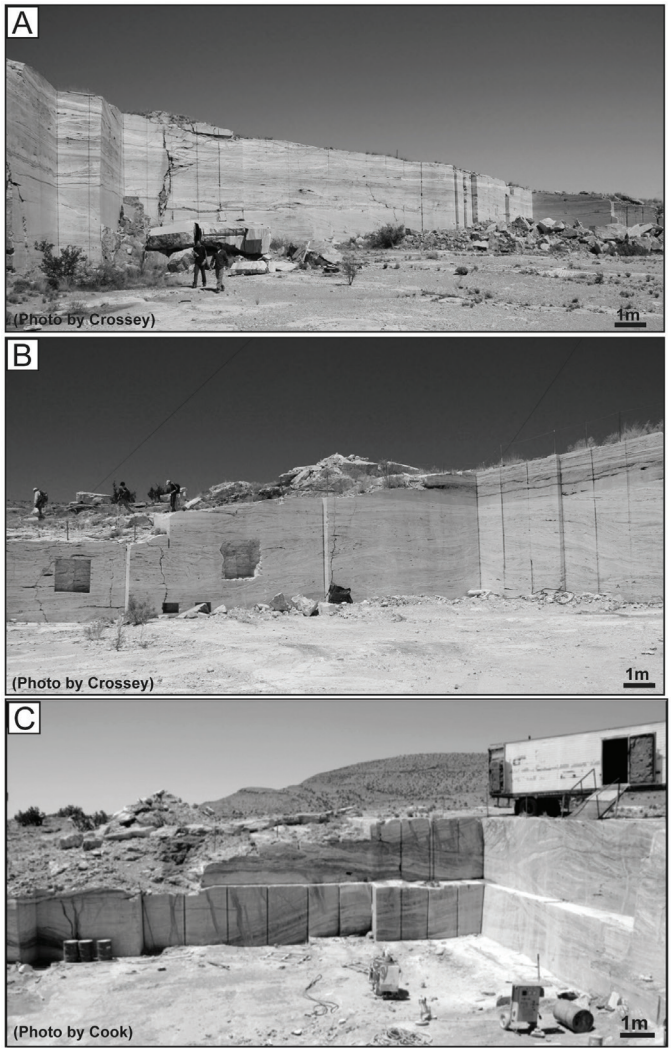


FIGURE 4. Views of the travertine quarries: Temple Cream (**A**), Scheherazade (**B**), and Vista Grande (**C**).

were dated and resulted in ages of older than 1.5 Ma (model age) and 245 ka (U-series age), respectively (Priewisch et al., 2014a). The quarry Scheherazade is located north of Temple Cream (Fig. 3). It is smaller and consists of reddish and white travertine (Fig. 4B). Two $^{234}$U-model ages of samples from a measured section at Scheherazade are 709 and 663 ka (Priewisch et al., 2014a). Vista Grande is the quarry farthest to the north (Fig. 3) and about the same size as Scheherazade (Fig. 4C). This quarry predominantly shows travertine veins varying in color from white, to beige, yellow, reddish, and brown (Fig. 4C). Two dated samples have ages of 560-690 ka (model ages) and 435 ka (U-series age; Priewisch et al., 2014a).

## METHODS

This section briefly describes the mapping of the travertine deposits, the macroscopic and microscopic facies analysis of selected hand specimen, and the analysis of stable oxygen and carbon isotopes of the travertine samples.

Mapping and geographic information system (GIS) volume analysis of travertine deposits at Mesa Aparejo was conducted on U.S. Geological Survey 7.5-minute topographic maps and RGIS (New Mexico Resource Geographic Information System) digital orthophotos (1 m resolution) in the field, and with ESRI (Environmental Systems Research Institute, Inc.) ArcGIS software as described in detail in Priewisch et al. (2014a). The areal extent of the travertine quarries was mapped by Ricketts et al. (2014).

A total of 49 travertine samples were collected by Priewisch (2014a) at the quarries Temple Cream (30 samples), Scheherazade (15 samples), and Vista Grande (4 samples). The oriented samples were taken along measured sections at each location. Hand specimens were cut into slabs to macroscopically evaluate different travertine facies and depositional environments. Microscopic thin section analysis was carried out by Cook (2013), who used float samples from the quarries for petrography. X-ray diffraction of samples was performed by Cook (2013) using a Siemens D5000 XRD at the University of Houston.

Powdered whole rock samples were drilled from calcite layers in travertine slabs. Between 0.5 mg and 1 mg of travertine powder was loaded in 12 mL borosilicate containers and flushed with helium and reacted with phosphoric acid at 50ºC for 24 hours. The evolved $CO_2$ was measured with a continuous flow Finnigan Mat Delta Plus Isotope Ratio Mass Spectrometer coupled to a Gasbench device. Results are reported in per mil (‰) using the delta notation versus PDB (Pee Dee Belemnite). Reproducibility is better than 0.15‰ for both $\delta^{13}C$ and $\delta^{18}O$ based on repeated measurements of a laboratory standard (Carrara Marble). The standard is calibrated versus NBS (National Bureau of Standards) 19, for which the $\delta^{13}C$ is 1.95‰ and $\delta^{18}O$ is 2.2‰. The samples were measured in the Center for Stable Isotopes, College of Arts & Sciences, University of New Mexico, using the method described by Spötl and Vennemann (2003).

Whole rock samples are commonly composed of more than one constituent. Research on different modern travertine systems has shown that different constituents within each system that formed within a few centimeters of each other can have systematically different stable isotopic values (see Fig. 9 in Chafetz and Lawrence, 1994). Thus, interpretations based on whole rock analyses, while commonly indicating valid trends, must be made with this caveat.

## RESULTS

### Travertine facies and their depositional environment

Based on field relationships and macroscopic petrographic analysis of the travertine samples from the quarries Temple Cream, Scheherazade, and Vista Grande, two main travertine facies can be distinguished: (1) terraced mound and sloping fan facies and (2) vein facies. The characteristic lithologies, fabrics, and depositional environments of each facies are described below, and a detailed facies description of individual samples is given in Table DR1. Excellent exposure of combined terraced mound and sloping fan and vein facies can be found at Temple Cream and Scheherazade, whereas Vista Grande predominantly displays the vein facies.

#### Terraced mound and sloping fan facies

Terraced mounds (e.g., Mammoth Hot springs Yellowstone National Park) form a series of horizontal pools separated by steeply-dipping to vertically-walled rimstone dams (Chafetz and Folk, 1984). Rimstone dams and their associated pools may range in size from several meters to centimeters or millimeters (Fig. 5A, B), whereas the relatively smooth sloping fans have less developed pool and rimstone dams (Fig. 5C) and are mainly represented by wedges of inclined layers from tens of centimeters to meters in thickness. Dams and pools on a centimeter and millimeter scale are termed microterracettes and cover the faces of steep dams (Fig. 6A/B; Fouke et al., 2000, 2003; Barth and Chafetz, 2015). The terraced mound facies consists of constituents such as peloids, coated grains, pisoids and oncoids, shrubs, travertine clasts and lithoclasts, travertine rafts, and calcified bubbles (Cook, 2013; Cook and Chafetz, 2014). Layers within the pools range from a few millimeters to several centimeters in thickness. The rimstone dams are composed of ray crystal crusts, a constituent observed in many travertine deposits (Folk et al., 1985; Guo and Chafetz, 2012). The color of the travertine varies from white, beige, reddish to brown (depending on iron and other trace element content), and the layers can be horizontal, wavy, irregular, or convoluted.

##### *Peloids, Coated Grains, Pisoids and Oncoids*

Peloids are round micritic particles of less than a millimeter to a few millimeters in size, whereas coated grains within these deposits are smaller (0.1-1 mm) and round in shape; they consist of a distinct nucleus and an even cortex of constant thickness (Fig. 7A-C; Pentecost, 2005; Cook, 2013). Pisoids and bacterial oncoids are round or elongate concentric grains that are usually several millimeters to a few centimeters large, consisting of a distinct nucleus and concentric but irregular cortices (Fig. 7D, E; Pentecost, 2005; Cook, 2013). The nucleus can be composed of either a clump of micrite or another constituent such as a travertine raft, the latter leading to elongate-shaped

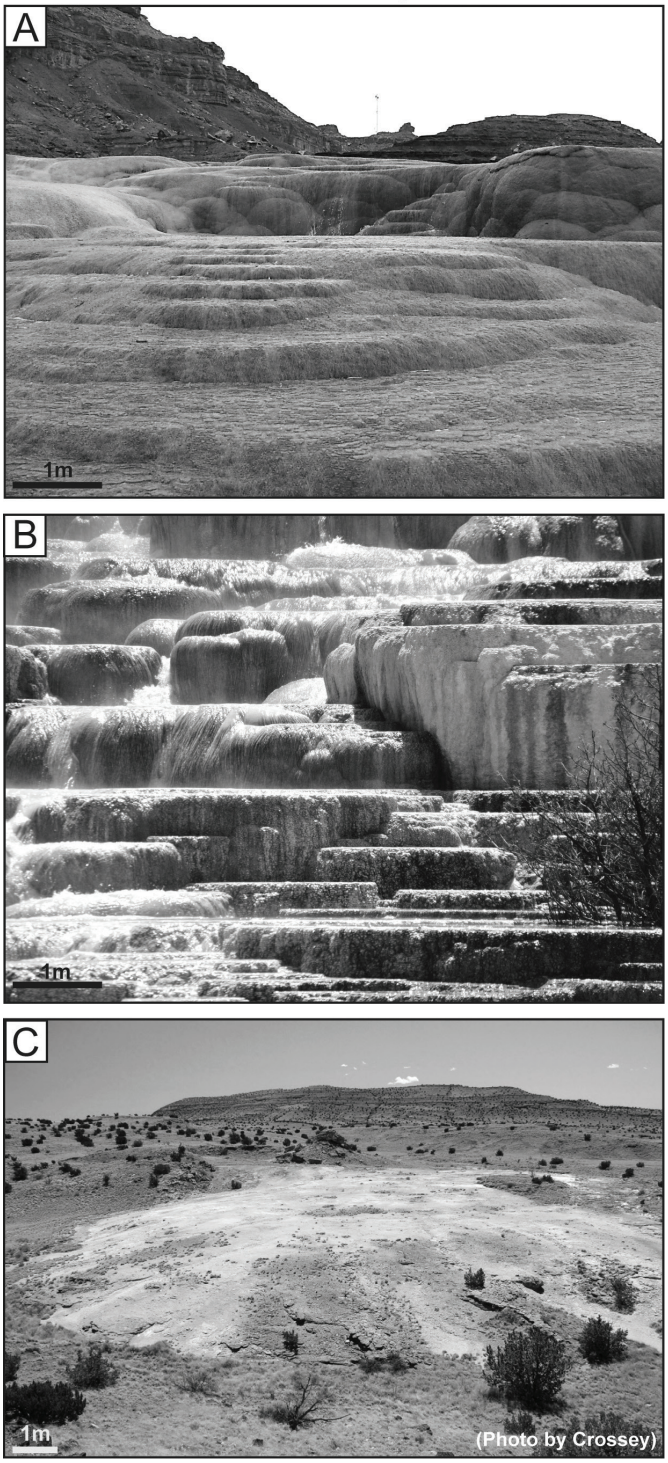


FIGURE 5. Examples of modern spring mounds. **A**) Terraced travertine mound at Crystal Geyser, Utah. **B**) Travertine terraces at Minerva Spring in Yellowstone National Park, Wyoming. **C**) Smooth spring mound north of the travertine quarries at Mesa Aparejo (view is towards the west); the modern travertine-precipitating Red Hill Spring (Figs. 2 and 3) is located northwest of the spring mound.

pisoids (Fig. 7D, E; Cook, 2013). Peloids, coated grains, and pisoids form at the bottom of pools, the latter accumulating adjacent to the rimstone dams (Chafetz and Folk, 1984; Guo and Riding, 1994; Pentecost, 2005).

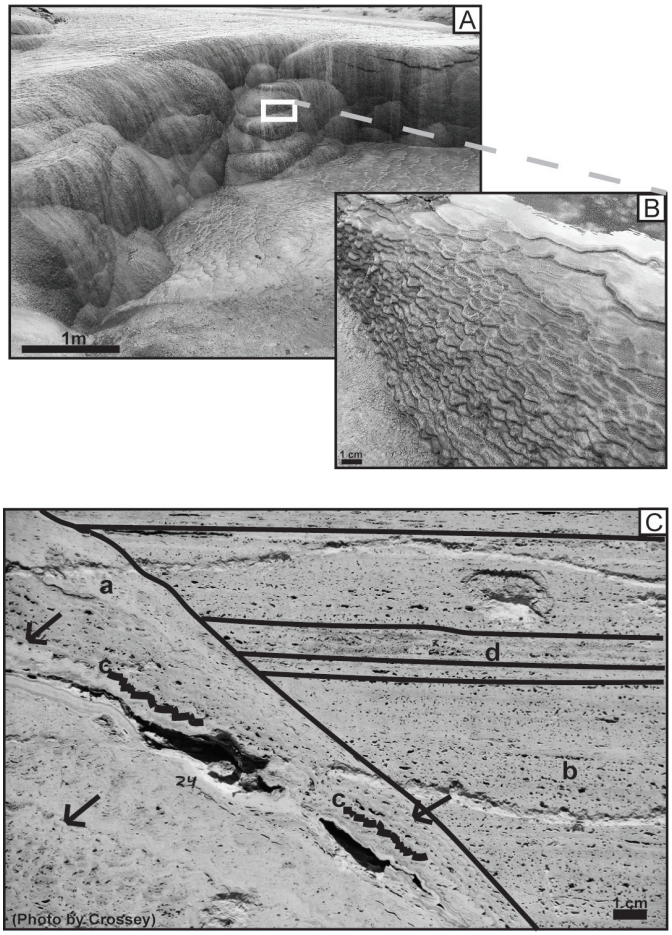


FIGURE 6. Examples of the terraced mound and sloping fan facies. **A**) Modern step-pools on the terraced travertine mound at Crystal Geyser, Utah. **B**) Close up of microterracettes on the steep slopes of a dam. **C**) Dam (a) and pool (b) exposed in a quarry wall at Temple Cream. Black arrows point to microterracettes which are also outlined in black (c). Horizontal layers representing the pool are also outlined in black (d).

### *Travertine Rafts*

Travertine rafts are thin, delicate crystalline layers that precipitate at the air-water interface in still water; continuing deposition thickens the raft and increases its mass until it sinks to the bottom of the pool (Pentecost, 2005). At Temple Cream, the length of rafts ranges from 0.7-3 mm and thickness varies between 0.1-0.8 mm (Fig. 7E, F; Cook, 2013).

### *Shrubs*

Shrubs are feathery or bush-like precipitates of either micrite or spar, which form due to bacterial or a combination of bacterial and abiotic processes at the bottom of pools (Fig. 8; Chafetz and Folk, 1984; Guo and Riding, 1998; Chafetz and Guidry, 1999). Bacterial shrubs at Temple Cream form laterally continuous layers of ~1 cm in thickness and consist of either single shrubs or multiple stacked shrubs; individual shrub layers are bounded by dense, peloidal layers (Fig. 8B; Cook, 2013).

### *Calcified Bubbles and Foam Rock*

Calcified bubbles are gas bubbles that get coated by rapidly precipitating calcium carbonate (Chafetz and Folk, 1984; Chafetz

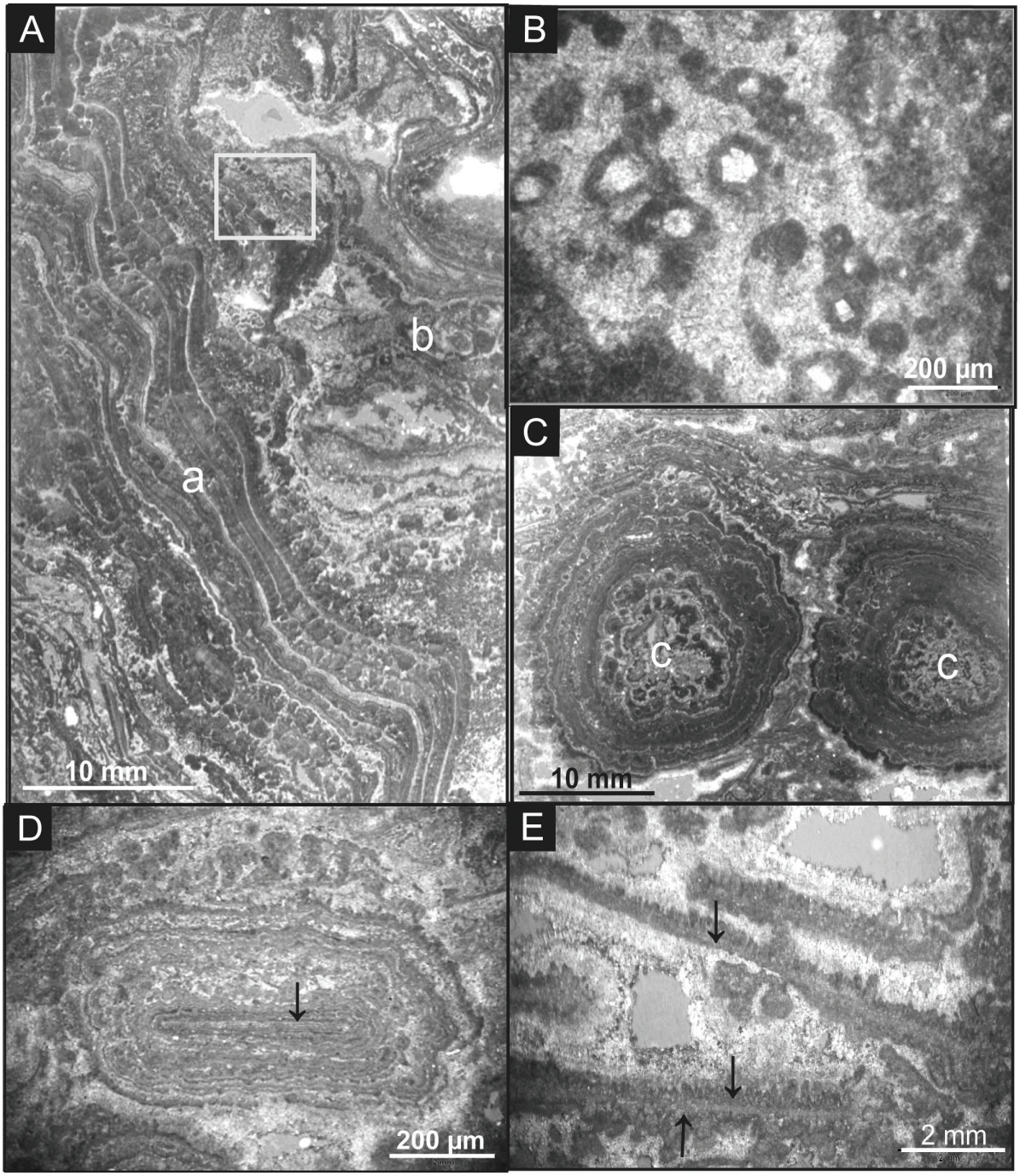


FIGURE 7. Photomicrographs of terraced mound and sloping fan facies (plain light; modified after Cook, 2013). **A**) Dam (a) and pool (b); grey box indicates locations of B). **B**) Coated grains, showing a single calcite crystal as nucleus and dark, micritic cortices that are slightly concentric, that accumulated in a pool adjacent to the dam. **C**) Spherical pisoids with micritic nuclei (c) and concentric but irregular cortices. **D**) Pisoid, oblate due to the shape of its nucleus (travertine raft; black arrow). **E**) Travertine rafts with isolated fan-shaped crusts (black arrows) on one or both sides of the raft.

et al., 1991a; Guo and Riding, 1998). If travertine consists mainly of elongated tubes formed by former gas bubbles, it is referred to as foam rock (Chafetz and Folk, 1984; Guo and Riding, 1998; Cook and Chafetz, 2014). At Temple Cream, foam rock layers range in thickness from 1-8 cm and either consist of a single row of tubes or multiple stacked tubes (Fig. 8D; Cook, 2013). Foam rock forms in pools and is associated with increased microbial activity (Chafetz and Folk, 1984; Guo and Riding, 1998).

### *Travertine Clasts and Lithoclasts*

Travertine clasts and lithoclasts are a few millimeters to several centimeters in size, the latter being clastic material such as sand grains or small pebbles, and both constituents occur as breccia or conglomerate. Pools and travertine surfaces can fall dry when discharge decreases or the rimstone dam is breached, which can lead to the formation of travertine crusts that may be reworked and broken up into travertine clasts. Lithoclasts are

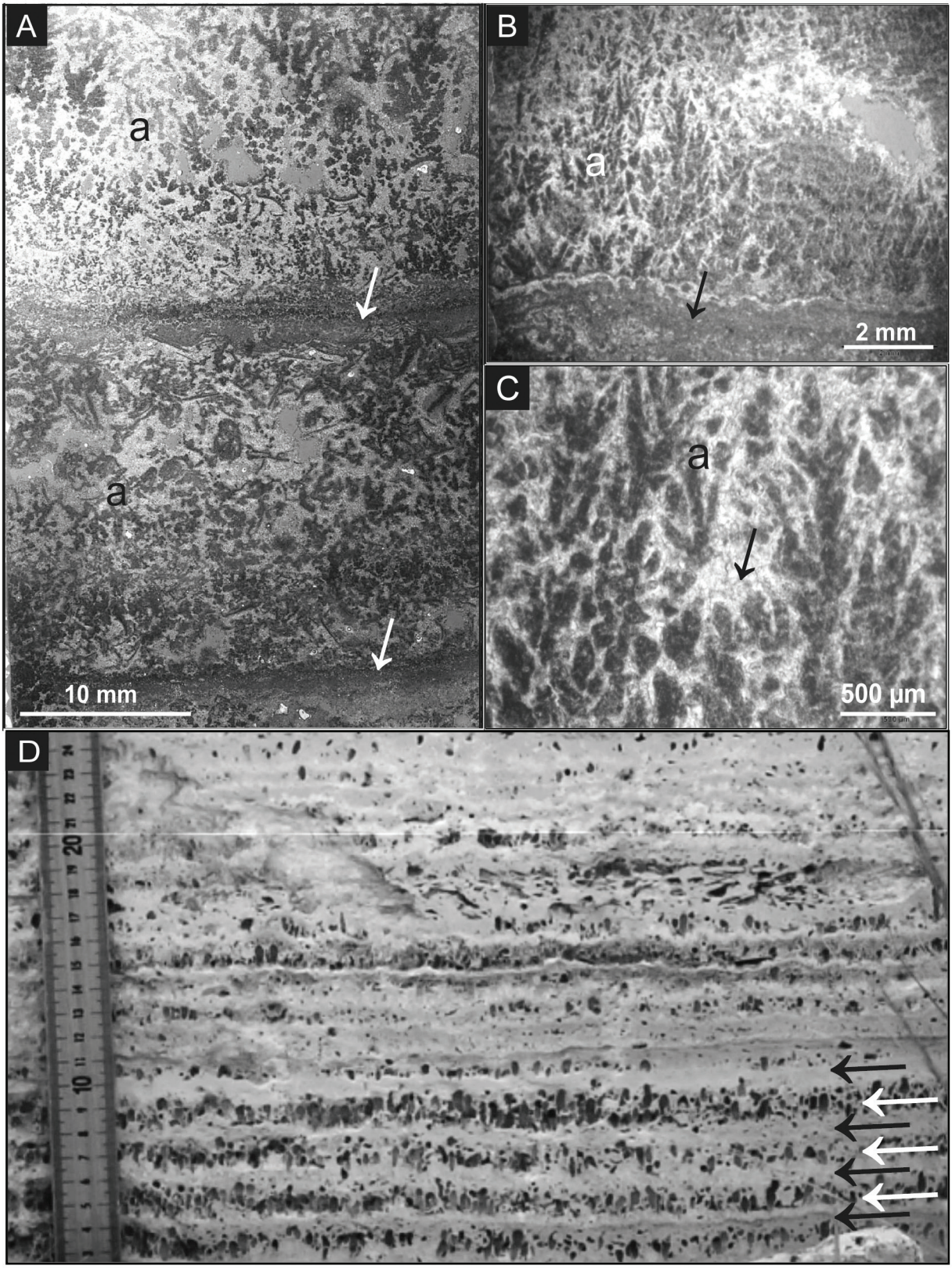


FIGURE 8. Photomicrographs of step-pool facies (plain light; modified after Cook, 2013). **A**) Bacterial shrub layers (a), separated by dense peloidal layers (white arrows). **B**) Close up of bacterial shrub layer (a) and dense peloidal layer (white arrow). **C**) Distinct bacterial shrub leaves (white arrows) surrounded by spar (black arrows). **D**) Horizontal micritic and foam rock layers representing a pool. Foam rock layers (white arrows) are separated by dense micrite layers (black arrows).

mostly limestone fragments which are washed into pools and onto travertine surfaces.

***Vein facies***

The vein facies is exceptionally well exposed at the quarry Vista Grande, although it also occurs at Temple Cream and Scheherazade. All analyzed samples from the Temple Cream and Scheherazade quarries are composed of calcite; however, some vein samples from other quarry locations are partly composed of aragonite (Cook, 2013). The vein facies consists of travertine-filled horizontal and vertical fractures a few millimeters to several tens of centimeters wide that cut across both older travertine and older veins (Fig. 9A). The travertine lithology predominantly consists of spar in different colors, e.g. white, grey, yellow, red, and brown, and white micrite (Fig. 9 B, C). Both spar and micrite veins are internally layered; individual layers range in size from 1-10 mm and can be horizontal, wavy, irregular, or convoluted (Fig. 9 B, C).

**Stable isotope analysis**

Stable oxygen and carbon isotopes of a total of 90 whole rock travertine samples from the three quarries were analyzed by Priewisch (Table DR2). Results overlap substantially, with a main range for $\delta^{13}C$ from +1.3‰ to +6.1‰ (Fig. 10A; Table DR2). Values of $\delta^{18}O$ range from -6.6‰ to -9.3‰.

At Temple Cream and Scheherazade, $\delta^{13}C$ values of the terraced mound and sloping fan facies range from +3.6‰ to +6.1‰ and +4.6‰ to +5.3‰, respectively (Fig. 10B; Table DR2). Values of $\delta^{18}O$ for the terraced mound and sloping fan facies are between -6.6‰ to -8.6‰ at Temple Cream and between -7.1‰ and -9.2‰ at Scheherazade (Fig. 10B; Table DR2). The spread of $\delta^{13}C$ values at Temple Cream is 2.5‰ and considerably wider than the spread of $\delta^{13}C$ values at Scheherazade, which is only 0.7‰, whereas the range of ~2‰ for the $\delta^{18}O$ values is basically the same for both quarries.

Most of the $\delta^{13}C$ values for the vein facies at Temple Cream are between +3.8‰ to +5.9‰, only one sample has a $\delta^{13}C$ value of +1.3‰ (Fig. 10C; Table DR2). At Scheherazade and Vista Grande, $\delta^{13}C$ values for the vein facies are between +4.1‰ and +5.6‰ and +3.7‰ and +5.7‰, respectively (Fig. 10C; Table DR2). Values of $\delta^{18}O$ range from -6.9‰ to -9.3‰ at Temple Cream, from -6.5‰ to -7.8‰ at Scheherazade, and from -6.5‰ to -9.3‰ at Vista Grande (Fig. 10C; Table DR2). The spread of $\delta^{13}C$ values at Temple Cream and Vista Grande is almost the same, ~2‰, whereas Scheherazade shows a smaller range of 1.5‰. Variations in $\delta^{18}O$ values are highest at Vista Grande with a spread of 2.8‰, followed by Temple Cream with a spread of 2.3‰, and are smallest at Scheherazade where the spread is only 1.3‰.

## DISCUSSION

This section provides an interpretation of the lateral and horizontal relationships between travertine facies, examines the stable isotopic composition of travertines according to facies, and investigates the amount of $CO_2$ and degassing rates that led to the formation of the large-volume travertine deposit at Mesa Aparejo.

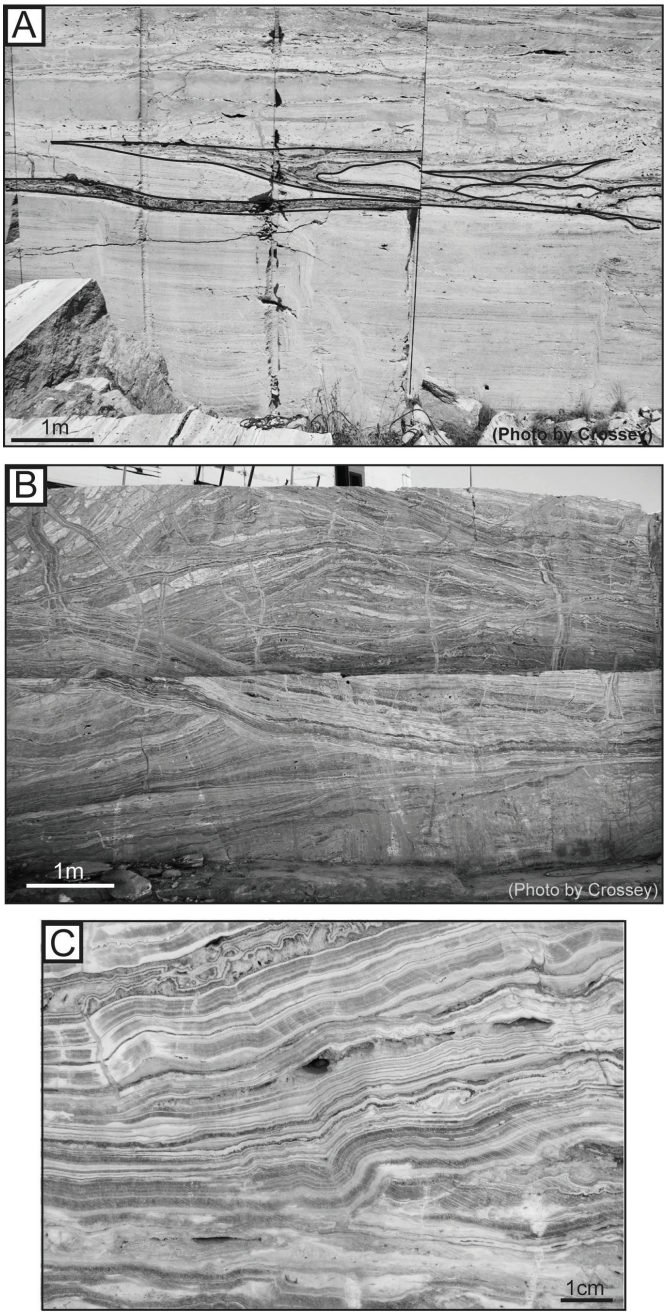


FIGURE 9. Examples of vein facies. **A**) Horizontal veins at Temple Cream (outlined in black). **B**) Different generations of horizontal and vertical veins at Vista Grande, cross-cutting each other. **C**) Wavy and convoluted veins at Vista Grande; the veins consist of both spar and micrite.

### Lateral and horizontal facies relationships

The quarries Temple Cream and Scheherazade provide excellent exposures of coalesced spring mounds, with predominantly terraced mounds at Temple Cream and mostly sloping fans at Scheherazade. Pools are represented by horizontal beds of travertine (Fig. 6C) that can contain travertine rafts, coated grains, peloids, pisoids, shrubs, and foam rock layers (Figs. 7, 8), whereas rimstone dams consist of inclined layers of ray crystal crusts that are often convoluted and lined by micro-

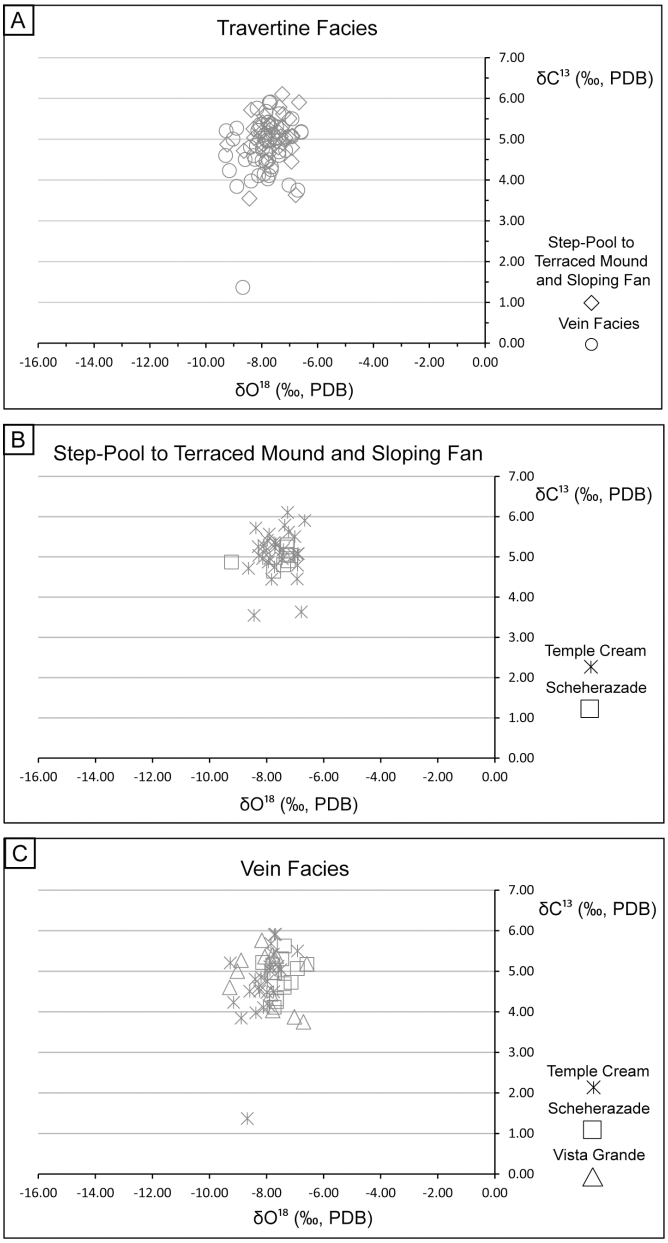


FIGURE 10. Stable isotope results from different travertine facies and different quarries. **A**) Stable isotope values of the terraced mound and sloping fan and vein facies for Temple Cream, Scheherazade, and Vista Grande. **B**) Comparison of stable isotope values of the terraced mound and sloping fan facies from Temple Cream and Scheherazade. C) Comparison of stable isotope values of the vein facies from Temple Cream, Scheherazade, and Vista Grande.

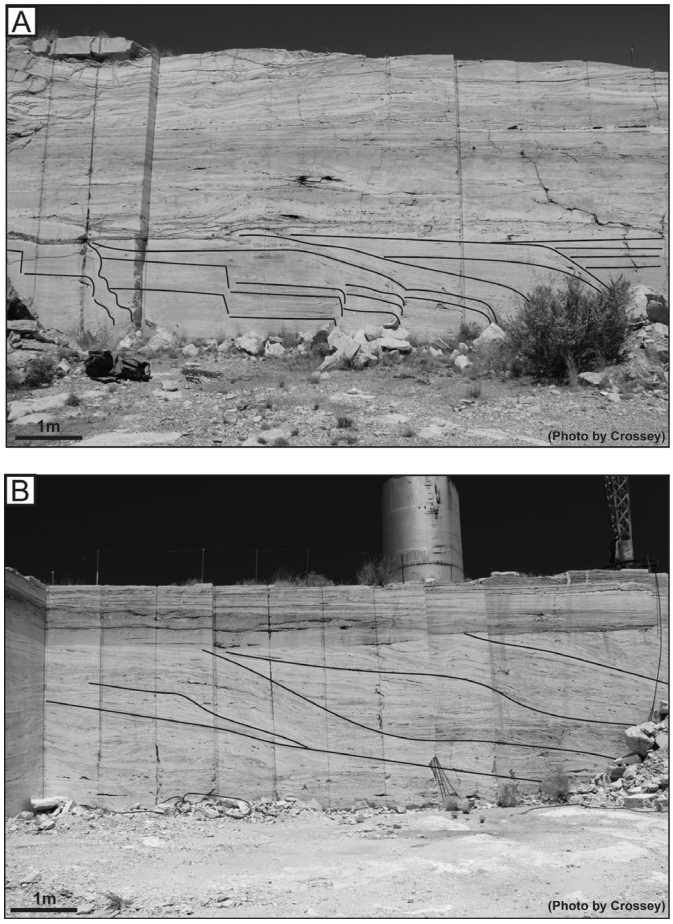


FIGURE 11. Examples of spring mounds in the rock record. **A**) Step-pool and sloping mound facies at Temple Cream, showing pools and dams of predominantly terraced spring mounds. Horizontal layers representing pools, wedges of inclined layers representing dams and sloping mounds are outlined in black. **B**) Step-pool and sloping mound facies at Scheherazade, showing wedges of inclined layers that mostly represent sloping mounds (outlined in black).

terracettes (Fig. 6C). The vertical record shows that the same pool consists of multiple stacked, horizontal travertine layers, whereas rimstone dams are built by multiple stacked inclined layers of ray crystal crusts (Fig. 11A). However, travertine deposits form in a highly dynamic depositional environment where spring vents migrate and pool and dam locations change. Various researchers (e.g., Fouke et al., 2000; Pentecost, 2005; Vylita et al., 2007; Linares et al., 2010; Fouke, 2011; Nishikawa et al., 2012) found that decrease or increase in groundwater head and discharge could cause active spring vents to fall dry and new spring vents to form in a new location, respectively. Continuous travertine precipitation or seismic activity along the fault might lead to sealing of an active spring vent or to reactivation of an inactive spring vent, respectively (Fouke et al., 2000; Pentecost, 2005; Vylita et al., 2007; Linares et al., 2010; Fouke, 2011; Nishikawa et al., 2012).

The rock record at Temple Cream shows that the rimstone dams and their associated pools migrated laterally, producing horizontal and vertical variations in the travertine deposits, and that terraced spring mounds transitioned into sloping fans (Fig. 11A). At Scheherazade, prograding wedges of travertine, which are composed of thick (tens of centimeters to meters) inclined layers, overlap each other due to vertical and lateral accretion of the sloping fans (Fig. 11B). During dry times when groundwater head was low and spring discharge ceased, terraces and travertine surfaces fell dry, broke into pieces and were then reworked when water flowed again, leading to the formation of travertine breccias, which now occur in distinct layers in the rock record. Lithoclasts have been transported by streams or debris flows from the nearby mountains onto the travertine

surfaces, sometimes intermixing with travertine clasts, which further contributed to the formation of breccia layers.

Vertical and horizontal veins cutting through the travertine deposits at Temple Cream, Scheherazade, and Vista Grande predominantly represent the plumbing system within the developing mounds, which facilitated both groundwater flow towards the surface and travertine precipitation. The vein facies formed in subsurface fractures within existing travertine deposits. Fracturing is related to extension of the Rio Grande rift and was likely induced by elevated fluid pressure of the $CO_2$-charged groundwater that flowed through the fractures (Sibson, 2000; Ricketts et al., 2014). Vertical veins represent the feeder system that conveyed deep groundwater to the surface, whereas horizontal veins represent fluid flow and artesian pressure exerted parallel to bedding (Uysal et al., 2007; De Filippis et al., 2012, 2013a, 2013b; Gratier et al., 2012). The abundance of veins increases from Temple Cream, to Scheherazade and Vista Grande, the latter displaying quarry walls that consist almost entirely of veins (Fig. 9B). Different generations of veins, that cross-cut not only the travertine deposits but also each other, indicate episodes of high groundwater head and abundant $CO_2$, leading to travertine precipitation within fractures.

## Interpretation of stable isotopic composition according to facies

The general overlap of stable isotope values of the terraced mound and sloping fan as well as the vein facies in the three quarries suggest that the composition and temperature of the water that these facies precipitated from may have been similar (Fig. 10A).

### Oxygen isotopes of the travertines

Controls on the oxygen isotopic composition of travertines, including composition and temperature of the groundwater source fluids, have been studied by various authors (e.g., Turi, 1986; Chafetz et al., 1991a; Chafetz et al., 1991b; Chafetz and Lawrence, 1994; Minissale et al., 2002b; Minissale, 2004; Newell et al., 2005; Crossey et al., 2006; Kele et al., 2011; Yan et al., 2012; Williams et al., 2013; Özkul et al., 2014; Sun et al., 2014; Wang et al., 2014). The $\delta^{18}O_c$ values are controlled by temperature and oxygen isotopic composition of the source water that precipitates the travertines. These conditions are in turn affected by 1) mixing of deeply-derived and shallow groundwater, 2) water-rock interactions along groundwater flow paths, 3) mixing of groundwater with meteoric water, and 4) evaporation. Mixing of groundwater and surface water as well as higher water temperature may lead to overall lower $\delta^{18}O$ values of the water ($\delta^{18}O_w$) and the travertine ($\delta^{18}O_c$), whereas lower water temperatures result in higher $\delta^{18}O_w$ and $\delta^{18}O_c$ values; evaporation and high travertine deposition rates cause higher $\delta^{18}O_c$ values (Gonfiantini et al., 1968; Turi, 1986; Chafetz et al., 1991a; Pentecost, 2005; Kele et al., 2011; Yan et al., 2012; Özkul et al., 2014; Sun et al., 2014; Wang et al., 2014).

The observed ranges of $\delta^{18}O$ values of the terraced mound and sloping fan facies and vein facies at the quarries Temple Cream, Scheherazade, and Vista Grande suggest that groundwater mixing (Priewisch et al., 2014b), mixing of groundwater and meteoric water, and changes in water temperature all played an important role during travertine precipitation (Fig. 10). The terraced mounds and sloping fans formed at the surface, which suggests that mixing of groundwater with meteoric water, evaporation, and variations in water temperature due to changing seasons as well as longer term changes in climate were likely controls of the oxygen isotopic composition, leading to the observed range of $\delta^{18}O$ values (Fig. 10B). The vein facies precipitated from groundwater flowing through subsurface fractures where mixing of deeply-derived and shallow groundwater likely played an important role. The observed different generations of veins likely represent travertine that precipitated from groundwater of different composition and temperature, which would explain the variations in $\delta^{18}O$ values for the three quarries (Fig. 10C).

Water temperatures of modern springs along the Comanche Fault (Fig. 2) vary between 6.1°C (Arroyo Salado Spring), 5.2°C and 4.1°C (Four Daughters springs), and $\delta^{18}O$ values of Four Daughters springs range from about -9.4‰ to about -10‰ (Blomgren et al., this volume). In order to estimate calcite-water-oxygen fractionation during travertine precipitation, $\delta^{18}O$ values of the paleowater were calculated based on the empirical equation of Demény et al. (2010). Calculated $\delta^{18}O$ values of the paleowater range between -13.8‰ and about -8‰ for water temperatures between 5°C and 20°C, respectively (Table DR3). The range of calculated $\delta^{18}O$ values at 20°C is closest to the range of $\delta^{18}O$ values of the modern spring water, which suggests that the paleowater temperature may have been higher than the present-day water temperature.

### Carbon isotopes of the travertines

The range of high $\delta^{13}C$ values for the three quarries is interpreted to be related to different rates of $CO_2$ degassing. The carbon isotopic composition of travertines is primarily controlled by the $CO_2$ degassing rate, which depends on: 1) partial pressure of $CO_2$, 2) water temperature, and 3) flow velocity (Groves and Howard, 1994; Howard and Groves, 1995; Hoffer-French and Herman, 1989; Qian et al., 2005; Hammer et al., 2007; Kele et al., 2011). Strong and turbulent degassing of $CO_2$ causes kinetic fractionation and isotopic disequilibrium, because the light carbon isotope $^{12}C$ will preferentially escape from solution, which leads to enrichment in the heavy carbon isotope $^{13}C$, and hence higher $\delta^{13}C$ values (Turi, 1986; Kele et al., 2011). Turbulent and laminar flow in fractures is likely important for the vein facies, because flow conditions impact $CO_2$ degassing rates, which increase towards the surface where decreasing pressure leads to strong $CO_2$ degassing (Groves and Howard, 1994; Howard and Groves, 1995; Hoffer-French and Herman, 1989; Qian et al., 2005; Hammer et al., 2007). $CO_2$ degassing is strongest in fast and turbulent flowing water (e.g., at rimstone dams), which leads to higher $\delta^{13}C$ values, whereas degassing rates are much lower from pools and ponds because the $pCO_2$ of the water has time to equilibrate with atmospheric $pCO_2$, which results in lower $\delta^{13}C$ values (Fuller et al., 2011; Kele et al., 2011; Yan et al., 2012; Wang et al., 2014).

At the modern Salado Arroyo Spring north of the Bel-

en quarries (Figs. 2, 3), the $\delta^{13}C$ value of the water is -1‰ (Blomgren et al., this volume). Assuming a similar $\delta^{13}C$ value for paleospring water that the travertine precipitated from, turbulent degassing could account for the high $\delta^{13}C$ values of the analyzed travertine samples. Another control on the carbon isotopic composition of travertines, particularly the terraced mound and sloping fan facies, is the presence of vegetation and microbiological activity. Both plants and microorganisms preferentially use the light carbon isotope, $^{12}C$, for photosynthesis and cell metabolic reactions, which lead to enrichment in $^{13}C$ and hence higher $\delta^{13}C$ values (Turi, 1986; Pentecost, 2005; Kele et al., 2011).

The considerably smaller range of $\delta^{13}C$ values at Scheherazade compared to Temple Cream is interpreted to reflect the presence of predominantly sloping fans at Scheherazade that lack well-developed pools and rimstone dams where strong $CO_2$ degassing would occur (Fig. 10B). Discharge was probably also lower at Scheherazade than at Temple Cream, where flow of turbulent water over terraced surfaces led to strong $CO_2$ degassing and a wider range of $\delta^{13}C$ values (Fig. 10B). The different generations of veins likely formed at different depths, below and within the existing travertine deposit, and reflect differing degrees of $CO_2$ degassing, which led to the observed range in $\delta^{13}C$ values for the three quarries (Fig. 10C). The veins with the highest $\delta^{13}C$ values are interpreted to have formed closest to the surface, whereas the veins with lower $\delta^{13}C$ values formed deeper in the subsurface (Fig. 10C).

### Amount of $CO_2$ and degassing rates

The presence of a large-volume travertine deposits such as that at Mesa Aparejo indicates that significant amounts of $CO_2$ must have degassed in order to precipitate such large volumes of travertine. Part of the $CO_2$ is mantle-derived or magmatic $CO_2$ (Hancock et al., 1999; Minissale et al., 2002b, 2005; Ballentine and Sherwood Lollar, 2002; Newell et al., 2005; Crossey et al., 2006, 2009; Embid, 2009; Karlstrom et al., 2013; Williams et al., 2013), and may have originated from the nearby Socorro magma body south of Mesa Aparejo (Figs. 1, 2; Ricketts et al., 2014). Modern travertine-depositing springs, including those near the Belen quarries (Figs. 2, 3), indicate that most of the $CO_2$ is derived from endogenic (deep) sources and $^3He/^4He$ ratios indicate that some of the helium is from the mantle (Hancock et al., 1999; Minissale et al., 2002b, 2005; Ballentine and Sherwood Lollar, 2002; Newell et al., 2005; Crossey et al., 2006, 2009; Embid, 2009; Karlstrom et al., 2013; Williams et al., 2013). At the Arroyo Salado Spring (Figs. 2, 3), for example, about 17.8% of the $CO_2$ is deeply derived, and a $^3He/^4He$ ratio of about 0.08% suggests that some of the helium originates in the mantle (Blomgren et al., this volume). Various basalt flows in the vicinity of Mesa Aparejo attest to repeated volcanic activity during the Quaternary (Figs. 1, 2; Baldridge et al., 1987; Dunbar, 2005; Ricketts et al., 2014), that would have contributed magmatic $CO_2$ to the groundwater system.

The amount of degassed $CO_2$ that led to the formation of the large-volume travertine deposit at Mesa Aparejo was estimated at 0.5 Gigatons (Gt), where half of the amount of $CO_2$ became fixed as travertine while the other half degassed into the atmosphere (Priewisch et al., 2014c). Considering that $CO_2$ also degassed along the fault system through carbonic springs and soil (Allis et al., 2005; Crossey et al., 2009; Karlstrom et al., 2013; Han et al., 2013; Smith et al., 2014), the estimated amount of degassed $CO_2$ is ~54 Gt over a time interval of ~456 ka (Priewisch et al., 2014c). These estimates support the view that the large-volume travertine deposit at Mesa Aparejo represents past degassing of a $CO_2$ gas reservoir (Priewisch et al., 2014a).

## CONCLUSIONS

Three travertine quarries located in the northwestern part of the large-volume deposit at Mesa Aparejo provide exceptional outcrops of terraced mound and sloping fan facies carbonates and vein facies carbonates that accumulated in coalescing travertine mounds and led to the formation of extensive travertine platforms. The terraced mound facies consist of pools represented by horizontal layers that often contain characteristic constituents (e.g., coated grains and shrubs), and the pools are separated by rimstone dams composed of ray crystal crusts. The sloping fan deposits are composed of inclined layers of varying thickness and steepness. The vein facies consists of travertine-filled fractures that opened due to rifting and elevated fluid pressures of $CO_2$-charged groundwater. The Temple Cream and Scheherazade quarries show predominantly coalesced terraced mounds and sloping fans with substantial lateral and vertical facies variations. Changes in $CO_2$ degassing rates, hydraulic head, and water composition were likely responsible for those variations. The travertine deposits at Temple Cream and Scheherazade are cut by several horizontal and a few vertical veins. The vein facies is exceptionally well exposed in the third quarry, Vista Grande, which was affected the most by extension and where multiple generations of horizontal and vertical veins cross-cut one another.

Results of stable isotope analyses show that facies have an effect on the geochemical composition of travertine. Values of $\delta^{18}O$ for the terraced mound and sloping fan and vein facies generally overlap, indicating that the travertine precipitated from groundwater of similar chemical composition. Values of $\delta^{13}C$ for the terraced mound and sloping fan facies differ slightly between Temple Cream and Scheherazade due to turbulent and less turbulent degassing of $CO_2$ on the terraced mounds and sloping fans, respectively. Values of $\delta^{13}C$ for the vein facies from the three quarries generally overlap, reflecting similar degassing rates in deep and shallow fractures.

It was necessary for considerable amounts of $CO_2$ to degas along the Comanche fault system to form the large-volume travertine deposit at Mesa Aparejo and the Socorro magma body might have provided the necessary magmatic $CO_2$. A degassing rate of ~54 Gt $CO_2$ over a period of 456 ka is estimated from the travertine archive, and stable isotope evidence suggests that substantial amounts of $CO_2$ degassed from the spring water into the atmosphere during carbon fractionation that accompanied travertine formation. This supports the hypothesis that the travertine deposit at Mesa Aparejo represents past degassing of a $CO_2$ reservoir (Priewisch et al., 2014a), possibly

associated with the Socorro magma body system.

## ACKNOWLEDGMENTS

We thank Jim Lardner of New Mexico Travertine, Inc., for access to the travertine quarries at Mesa Aparejo, Alexander Nereson and Jason Ricketts for invaluable field assistance, Rebecca Wacker for preparing the travertine samples for stable isotope analysis, and Viorel Atudorei of the Stable Isotope Center at the University of New Mexico for help and advice. We thank Bruce Allen and Robert Riding for valuable edits, which helped greatly to improve this paper. Funding for this study was provided by National Science Foundation (NSF) EAR-0838575 (to Crossey), American Association of Petroleum Geologists Grants-In-Aid, New Mexico Geological Society grants-in-aid, and Graduate and Professional Student Association of the University of New Mexico.

## REFERENCES

Ake, J.P., and Sanford, A.R., 1988, New evidence for the existence and internal structure of a thin layer of magma at mid-crustal depths near Socorro, New Mexico: Bulletin of the Seismological Society of America, v. 78, p. 1335–1359.

Aldrich, M.J., 1986, Tectonics of the Jemez lineament in the Jemez Mountains and Rio Grande rift: Journal of Geophysical Research, v. 91, p. 1753–1762.

Allis, R., Bergfeld, D., Moore, J., McClure, K., Chidsey, T., Heath, J., and Mcpherson, B., 2005, Implications of results from $CO_2$ flux surveys over known $CO_2$ systems for long-term monitoring, *in* Alexandria, Fourth Annual Conference on Carbon Capture & Sequestration, p. 1–22.

Andrews, J.E., 2006, Palaeoclimatic records from stable isotopes in riverine tufas: synthesis and review: Earth-Science Reviews, v. 75, p. 85–104, doi: 10.1016/j.earscirev.2005.08.002.

Andrews, J.E., Pedley, M., and Dennis, P.F., 2000, Palaeoenvironmental records in Holocene Spanish tufas: a stable isotope approach in search of reliable climatic archives: Sedimentology, v. 47, p. 961–978, doi: 10.1046/j.1365-3091.2000.00333.x.

Anzalone, E., Ferreri, V., Sprovieri, M., and D'Argenio, B., 2007, Travertines as hydrologic archives: the case of the Pontecagnano deposits (southern Italy): Advances in Water Resources, v. 30, p. 2159–2175, doi: 10.1016/j.advwatres.2006.09.008.

Austin, G.S., and Barker, J.M., 1990, Commercial travertine in New Mexico: New Mexico Geology, v. 12, p. 49–58.

Balch, R.S., Hartse, H.E., Sanford, A.R., and Lin, K. -w., 1997, A new map of the geographic extent of the Socorro mid-crustal magma body: Bulletin of the Seismological Society of America, v. 87, p. 174–182.

Baldridge, W.S., Perry, F.V., and Shafiqullah, M., 1987, Late Cenozoic volcanism of the southeastern Colorado Plateau: I. Volcanic geology of the Lucero area, New Mexico: Geological Society of America Bulletin, v. 99, p. 463–470.

Ballentine, C.J., and Sherwood Lollar, B., 2002, Regional groundwater focusing of nitrogen and noble gases into the Hugoton-Panhandle giant gas field, USA: Geochimica et Cosmochimica Acta, v. 66, p. 2483–2497.

Barker, J.M., Austin, G.S., and Sivils, D.J., 1996, Travertine in New Mexico - Commercial deposits and otherwise: New Mexico Bureau of Mines and Mineral Resources Bulletin, v. 154, p. 73–92.

Barth, J.A., and Chafetz, H.S., 2015, Cool water geyser travertine: Crystal Geyser, Utah, USA: Sedimentology, v. 62, p. 607–620, doi: 10.1111/sed.12158.

Blomgren, V., Williams, A.J., Crossey, L.J., Karlstrom, K.E., and McGibbon, C., 2016, Identifying the sources of $CO_2$ in carbonic springs in the Albuquerque-Belen Basin: New Mexico Geological Society, Guidebook 67, p. 419-427.

Callender, J., and Zilinski, Jr, R., 1976, Kinematics of Tertiary and Quaternary deformation along the eastern edge of the Lucero uplift, central New Mexico, *in* Woodward, L.A. and Northrop, S.A. eds., Tectonics and Mineral Resources of Southwestern North America: New Mexico Geological Society, p. 53–61.

Cather, S.M., 2004, Laramide orogeny in central and northern New Mexico and southern Colorado, *in* Mack, G.H. and Giles, K.A. eds., The Geology of New Mexico: New Mexico Geological Society Special Publication 11, p. 203–248.

Chafetz, H.S., and Folk, R.L., 1984, Travertines; depositional morphology and the bacterially constructed constituents: Journal of Sedimentary Petrology, v. 54, p. 289–316.

Chafetz, H.S., and Guidry, S.A., 1999, Bacterial shrubs , crystal shrubs and ray-crystal shrubs: bacterial versus abiotic precipitation: Sedimentary Geology, v. 126, p. 57–74.

Chafetz, H.S., and Lawrence, J.R., 1994, Stable Isotopic Variability Within: Geographie physique et Quaternaire, v. 48, p. 257–273, doi: 10.7202/033007ar.

Chafetz, H.S., Rush, P.F., and Utech, N.M., 1991, Microenvironmental controls on mineralogy and habit of CaCO3 precipitates: an example from an active travertine system: Sedimentology, v. 38, p. 107–126.

Chafetz, H.S., Utech, N.M., and Fitzmaurice, S.P., 1991, Differences in the δ18O and δ13C Signatures of Seasonal Laminae Comprising Travertine Stromatolites: Journal of Sedimentary Petrology, v. 61, p. 1015–1028, doi: 10.1306/D426782A-2B26-11D7-8648000102C1865D.

Chamberlin, R.M., 2007, Evolution of the Jemez lineament: connecting the volcanic "dots" through late cenozoic time: New Mexico Geological Society, Guidebook 58, p. 80–82.

Cook, M.A., 2013, Lateral and Temporal Facies Variations in a Quaternary Travertine Deposit, Belen, New Mexico [M.S. thesis]: Houston, University of Housten, 143 p.

Cook, M.A., and Chafetz, H.S., 2014, Transitional terraced mound to sloping mound facies relationships of a Quaternary travertine quarry in Belen, New Mexico: AAPG Datapages/Search and Discovery Article #90189, AAPG Annual Convention and Exhibition, Houston, Texas, USA, April 6–9, 2014.

Cron, B., 2011, Geochemical characteristics and microbial diversity of $CO_2$-rich mound springs of the Tierra Amarilla anticline, New Mexico [M.S. thesis]: Albuquerque, University of New Mexico, 110 p.

Crossey, L.J., Fischer, T.P., Patchett, P.J., Karlstrom, K.E., Hilton, D.R., Newell, D.L., Huntoon, P., Reynolds, A.C., and de Leeuw, G.A.M., 2006, Dissected hydrologic system at the Grand Canyon: Interaction between deeply derived fluids and plateau aquifer waters in modern springs and travertine: Geology, v. 34, p. 25–28, doi: 10.1130/G22057.1.

Crossey, L.J., Karlstrom, K.E., Newell, D.N., Kooser, A., and Tafoya, A., 2011, The La Madera travertines, Rio Ojo Caliente, northern New Mexico : Investigating the linked system of $CO_2$-rich springs and travertines as neotectonic and paleoclimate indicators, *in* New Mexico Geological Society, Guidebook 62, p. 121–136.

Crossey, L.J., Karlstrom, K.E., Springer, A.E., Newell, D., Hilton, D.R., and Fischer, T., 2009, Degassing of mantle-derived $CO_2$ and He from springs in the southern Colorado Plateau region--Neotectonic connections and implications for groundwater systems: Geological Society of America Bulletin, v. 121, p. 1034–1053, doi: 10.1130/B26394.1.

De Filippis, L., Anzalone, E., Billi, A., Faccenna, C., Poncia, P.P., and Sella, P., 2013a, The origin and growth of a recently-active fissure ridge travertine over a seismic fault, Tivoli, Italy: Geomorphology, v. 195, p. 13–26, doi: 10.1016/j.geomorph.2013.04.019.

De Filippis, L., Faccenna, C., Billi, A., Anzalone, E., Brilli, M., Soligo, M., and Tuccimei, P., 2013b, Plateau versus fissure ridge travertines from Quaternary geothermal springs of Italy and Turkey: Interactions and feedbacks between fluid discharge, paleoclimate, and tectonics: Earth-Science Reviews, v. 123, p. 35–52, doi: 10.1016/j.earscirev.2013.04.004.

De Filippis, L., Faccenna, C., Billi, A., Anzalone, E., Brilli, M., Ozkul, M., Soligo, M., Tuccimei, P., and Villa, I.M., 2012, Growth of fissure ridge travertines from geothermal springs of Denizli Basin, western Turkey: Geological Society of America Bulletin, v. 124, p. 1629–1645, doi: 10.1130/B30606.1.

Demeny, A., Kele, S., and Siklosy, Z., 2010, Empirical equations for the temperature dependence of calcite-water oxygen isotope fractionation from 10 to 70 C: Rapid Communications in Mass Spectrometry, v. 24, p. 3521–3526, doi: 10.1002/rcm.

Dunbar, N., 2005, Quaternary volcanism in New Mexico: New Mexico Museum of Natural History and Science Bulletin, v. 28, p. 95–106, http://

geoinfo.nmt.edu/staff/dunbar/publications/abstracts/Dunbar2005.pdf (accessed January 2013).

Embid, E.H., 2009, U-Series dating, geochemistry, and geomorphic studies of travertines and springs ot the Springerville Area, east-central Arizona, and tectonic implications [M.S. thesis]: Albuquerque, University of New Mexico, 103 p.

Faccenna, C., Soligo, M., Billi, A., De Filippis, L., Funiciello, R., Rossetti, C., and Tuccimei, P., 2008, Late Pleistocene depositional cycles of the Lapis Tiburtinus travertine (Tivoli, Central Italy): possible influence of climate and fault activity: Global and Planetary Change, v. 63, p. 299–308, doi: 10.1016/j.gloplacha.2008.06.006.

Feth, J.H., and Barnes, I., 1979, Spring-deposited travertine in eleven western states: Geological Survey Water-Resources Investigations 79-85 Open-File Report, v. Open-File.

Fialko, Y., and Simons, M., 2001, Evidence for on-going inflation of the Socorro Magma Body, New Mexico, from Interferometric Synthetic Aperture Radar imaging: Geophysical Research Letters, v. 28, p. 3549–3552, doi: 10.1029/2001GL013318.

Folk, R.L., Chafetz, H.S., and Tiezzi, P.A., 1985, Bizarre forms of depositional and diagenetic calcite in hot-spring travertines, central Italy: Carbonate Cements, p. 349–369.

Ford, T.D., and Pedley, H.M., 1996, A review of tufa and travertine deposits of the world: Earth-Science Reviews, v. 41, p. 117–175.

Fouke, B.W., 2011, Hot-spring Systems Geobiology: abiotic and biotic influences on travertine formation at Mammoth Hot Springs, Yellowstone National Park, USA: Sedimentology, v. 58, p. 170–219, doi: 10.1111/j.1365-3091.2010.01209.x.

Fouke, B.W., Bonheyo, G.T., Sanzenbacher, B., and Frias-Lopez, J., 2003, Partitioning of bacterial communities between travertine depositional facies at Mammoth Hot Springs, Yellowstone National Park, U.S.A . 1: Canadian Journal of Earth Sciences, v. 40, p. 1531–1548, doi: 10.1139/E03-067.

Fouke, B.W., Farmer, J.D., Des Marais, D.J., Pratt, L., Sturchio, N.C., Burns, P.C., and Discipulo, M.K., 2000, Depositional facies and aqueous-solid geochemistry of travertine-depositing hot springs (Angel Terrace, Mammoth Hot Springs, Yellowstone National Park, U.S.A.): Journal of Sedimentary Research, v. 70, p. 565–585, http://www.ncbi.nlm.nih.gov/pubmed/11543518.

Fuller, B.M., Sklar, L.S., Compson, Z.G., Adams, K.J., Marks, J.C., and Wilcox, A.C., 2011, Ecogeomorphic feedbacks in regrowth of travertine step-pool morphology after dam decommissioning, Fossil Creek, Arizona: Geomorphology, v. 126, p. 314–332, doi: 10.1016/j.geomorph.2010.05.010.

Glover, C., and Robertson, A.H.F., 2003, Origin of tufa (cool-water carbonate) and related terraces in the Antalya area, SW Turkey: Geological Journal, v. 38, p. 329–358, doi: 10.1002/gj.959.

Goff, F., McCormick, T., Gardner, J.N., Trujillo, P.E., Counce, D., Vidale, R., and Charles, R., 1983, Water geochemistry of the Lucero uplift, New Mexico: A geothermal investigation of low-temperature mineralized fluids: Los Alamos National Laboratory LA-9738-OBES, 26 p., 26 p.

Gonfiantini, R., Panichi, C., and Tongiorgi, E., 1968, Isotopic disequilibrium in travertine deposition: Earth and Planetary Science Letters, v. 5, p. 55–58.

Gratier, J.-P., Frery, E., Deschamps, P., Royne, A., Renard, F., Dysthe, D., Ellouz-Zimmerman, N., and Hamelin, B., 2012, How travertine veins grow from top to bottom and lift the rocks above them: The effect of crystallization force: Geology, p. 1–4, doi: 10.1130/G33286.1.

Groves, G., and Howard, A.D., 1994, Early develpment of karst systems: 1. Preferential flow path enlargement under laminar flow: v. 30, p. 2837–2846.

Guo, X., and Chafetz, H.S., 2012, Large tufa mounds, Searles Lake, California: Sedimentology, v. 59, p. 1509–1535, doi: 10.1111/j.1365-3091.2011.01315.x.

Guo, L., and Riding, R., 1994, Origin and diagenesis of Quternary travertine shrub fabrics, Rapolano Terme, central Italy: Sedimentology, v. 41, p. 499–520.

Guo, L., and Riding, R., 1998, Hot-spring travertine facies and sequences, Late Pleistocene, Rapolano Terme, Italy: Sedimentology, v. 45, p. 163–180.

Guo, L.I., and Riding, R., 1999, Rapid facies changes in Holocene fissure ridge hot spring travertines, Rapolano Terme, Italy: Sedimentology, v. 46, p. 1145–1158.

Hammer, O., Dysthe, D., and Jamtveit, B., 2007, The dynamics of travertine dams: Earth and Planetary Science Letters, v. 256, p. 258–263, doi: 10.1016/j.epsl.2007.01.033.

Han, W.S., Lu, M., McPherson, B.J., Keating, E.H., Moore, J., Park, E., Watson, Z.T., and Jung, N.-H., 2013, Characteristics of $CO_2$-driven cold-water geyser, Crystal Geyser in Utah: experimental observation and mechanism analyses: Geofluids, v. 13, p. 283–297.

Hancock, P.L., Chalmers, R.M.., Altunel, E., and Cakir, Z., 1999, Travitonics: using travertines in active fault studies: Journal of Structural Geology, v. 21, p. 903–916.

Hoffer-French, K.J., and Herman, J.S., 1989, Evaluation of hydrological and biological influences on $CO_2$ fluxes from a karst system: Journal of Hydrology, v. 108, p. 189–212.

Howard, A.D., and Groves, C.G., 1995, Early develpment of karst systems: 2. Turbulent flow: Water Resources Research, v. 31, p. 19–26.

Jones, B., and Renaut, R.W., 2010, Calcareous spring deposits in continental settings, *in* Alonso-Zara, A.M. and Tanner, L.H. eds., Carbonates in Continental Settings: Amsterdam, Elsevier, Developments in Sedimentology 61, p. 177–224.

Kampman, N., Burnside, N.M., Shipton, Z.K., Chapman, H.J., Nicholl, J.A., Ellam, R.M., and Bickle, M.J., 2012, Pulses of carbon dioxide emissions from intracrustal faults following climatic warming: Nature Geoscience, v. 5, p. 352–358, doi: 10.1038/ngeo1451.

Karlstrom, K.E., Crossey, L.J., Hilton, D.R., and Barry, P.H., 2013, Mantle 3He and $CO_2$ degassing in carbonic and geothermal springs of Colorado and implications for neotectonics of the Rocky Mountains: Geology, v. 41, p. 495–498, doi: 10.1130/G34007.1.

Kele, S., Demény, A., Siklósy, Z., Németh, T., Tóth, M., and Kovács, M.B., 2008, Chemical and stable isotope composition of recent hot-water travertines and associated thermal waters, from Egerszalók, Hungary: Depositional facies and non-equilibrium fractionation: Sedimentary Geology, v. 211, p. 53–72, doi: 10.1016/j.sedgeo.2008.08.004.

Kele, S., Özkul, M., Fórizs, I., Gökgöz, A., Baykara, M.O., Alçiçek, M.C., and Németh, T., 2011, Stable isotope geochemical study of Pamukkale travertines: new evidences of low-temperature non-equilibrium calcite-water fractionation: Sedimentary Geology, v. 238, p. 191–212, doi: 10.1016/j.sedgeo.2011.04.015.

Keller, G.R., and Baldridge, W.S., 1999, The Rio Grande rift A geological and geophysical overview: Rocky Mountain Geology, v. 34, p. 121–130.

Linares, R., Rosell, J., Roqué, C., and Gutiérrez, F., 2010, Origin and evolution of tufa mounds related to artesian karstic springs in Isona area (Pyrenees, NE Spain): Geodinamica Acta, v. 23, p. 129–150, doi: 10.3166/ga.23.129-150.

Minissale, A., 2004, Origin, transport and discharge of $CO_2$ in central Italy: Earth-Science Reviews, v. 66, p. 89–141, doi: 10.1016/j.earscirev.2003.09.001.

Minissale, A., Kerrick, D.M., Magro, G., Murrell, M.T., Paladini, M., Rihs, S., Sturchio, N.C., Tassi, F., and Vaselli, O., 2002a, Geochemistry of Quaternary travertines in the region north of Rome (Italy): structural, hydrologic and paleoclimatic implications: Earth and Planetary Science Letters, v. 203, p. 709–728.

Minissale, A., Paladini, M., and Sturchio, N.C., 2005, Travertine of central Italy: relation between genesis, tectonics and paleoclimate: Proceedings of the 1st International Symposium on Travertine, p. 106–115.

Minissale, A., Vaselli, O., Tassi, F., Magro, G., and Grechi, G.P., 2002b, Fluid mixing in carbonate aquifers near Rapolano (central Italy): chemical and isotopic constraints: Applied Geochemistry, v. 17, p. 1329–1342.

Minor, S.A., Hudson, M.R., Cain, J.S., and Thompson, R.A., 2013, Oblique transfer of extensional strain between basins of the middle Rio Grande rift, New Mexico: Fault kinematic and paleostress constraints, *in* Hudson, M.R. and Grauch, V.J.S. (Tien) eds., New Perspectives on Rio Grande Basins: From Tectonics to Groundwater: The Geological Society of America Special Paper 494, p. 345–382.

New Mexico Bureau of Geology and Mineral Resources, 2003, Geologic Map of New Mexico: New Mexico Bureau of Geology and Mineral Resources, scale 1:500 000, 2 sheets.

Newell, D.L., Crossey, L.J., Karlstrom, K.E., Fischer, T.P., and Hilton, D.R., 2005, Continental-scale links between the mantle and groundwater systems of the western United States: Evidence from travertine springs and regional He isotope data: GSA Today, v. 15, p. 4–10.

Nishikawa, O., Furuhashi, K., Masuyama, M., Ogata, T., Shiraishi, T., and Shen, C.C., 2012, Radiocarbon dating of residual organic matter in travertine formed along the Yumoto Fault in Oga Peninsula, northeast Ja-

pan: Implications for long-term hot spring activity under the influence of earthquakes: Sedimentary Geology, v. 243-244, p. 181–190, doi: 10.1016/j.sedgeo.2011.11.001.

Özkul, M., Gökgöz, A., Kele, S., Baykara, M.O., Shen, C.-C., Chang, Y.-W., Kaya, A., Hançer, M., Aratman, Ci., Akin, T., and Örü, Z., 2014, Sedimentological and geochemical characteristics of a fluvial travertine: A case from the eastern Mediterranean region (E. Capezzuoli, Ed.): Sedimentology, v. 61, p. 291–318, doi: 10.1111/sed.12095.

Pearse, J., and Fialko, Y., 2010, Mechanics of active magmatic intraplating in the Rio Grande Rift near Socorro, New Mexico: Journal of Geophysical Research, v. 115, p. 1–16, doi: 10.1029/2009JB006592.

Pedley, H.M., 1990, Classification and environmental models of cool freshwater tufas: Sedimentary Geology, v. 68, p. 143–154.

Pedley, H.M., 2009, Tufas and travertines of the Mediterranean region: a testing ground for freshwater carbonate concepts and developments: Sedimentology, v. 56, p. 221–246, doi: 10.1111/j.1365-3091.2008.01012.x.

Pentecost, A., 2005, Travertine: Berlin, Springer Verlag, 445 p.

Pentecost, A., and Viles, H., 1994, A review and reassessment of travertine classification: Geographie physique et Quaternaire, v. 48, p. 305–314.

Priewisch, A., Crossey, L.J., Karlstrom, K.E., Polyak, V.J., Asmerom, Y., Nereson, A., and Ricketts, J.W., 2014a, U-series geochronology of large-volume Quaternary travertine deposits of the southeastern Colorado Plateau: Evaluating episodicity and tectonic and paleohydrologic controls: Geosphere, v. 10, p. 401–423, doi: 10.1130/GES00946.1.

Priewisch, A., Crossey, L.J., Karlstrom, K.E., and Mozley, P.S., 2014b, Evaluating Quaternary travertine deposits of the Rio Grande rift and Colorado Plateau: Geochemical signatures of travertine facies and quantification of long-term $CO_2$ leakage along faults, with implications for $CO_2$ sequestration.: New Mexico Geological Society Annual Spring Meeting, Proceedings Volume, p. 51.

Priewisch, A., Crossey, L.J., Karlstrom, K.E., and Mozley, P.S., 2014c, Extensive $CO_2$ leakage from extinct and modern $CO_2$ reservoirs in New Mexico and Arizona: Evaluating the role of seal bypass and large-volume travertine deposition with implications for $CO_2$ sequestration: American Geophysical Union Fall Meeting.

Qian, J., Zhan, H., Zhao, W., and Sun, F., 2005, Experimental study of turbulent unconfined groundwater flow in a single fracture: Journal of Hydrology, v. 311, p. 134–142, doi: 10.1016/j.jhydrol.2005.01.013.

Reiter, M., Chamberlin, R.M., and Love, D.W., 2010, New data reflect on the thermal antiquity of the Socorro magma body locale, Rio Grande Rift, New Mexico: Lithosphere, v. 2, p. 447–453, doi: 10.1130/L115.1.

Ricketts, J.W., Karlstrom, K.E., Priewisch, A., Crossey, L.J., Polyak, V.J., and Asmerom, Y., 2014, Quaternary extension in the Rio Grande rift at elevated strain rates recorded in travertine deposits, central New Mexico: Lithosphere, v. 6, p. 3–16, doi: 10.1130/L278.1.

Rinehart, E.J., and Sanford, A.R., 1981, Upper crustal structure of the Rio Grande rift near Socorro, New Mexico, from inversion of microearthquake S-wave reflections: Bulletin of the Seismological Society of America, v. 71, p. 437–450.

Seager, W., 2004, Laramide (Late Cretaceous-Eocene) tectonics of southwestern New Mexico, *in* Mack, G.H. and Giles, K.A. eds., The Geology of New Mexico, New Mexico Geological Society Special Publication 11, p. 183–202.

Sibson, R.H., 2000, Fluid involvement in normal faulting: Journal of Geodynamics, v. 29, p. 469–499, doi: 10.1016/S0264-3707(99)00042-3.

Smith, J., Crossey, L.J., Karlstrom, K.E., Fischer, T.P., Lee, H., and McGibbon, C., 2014, Fault networks in the northwestern Albuquerque Basin and their potential role in controling mantle $CO_2$ degassing and fluid migration from the Valles Caldera: American Geophysical Union Fall Meeting.

Smith, J.R., Giegengack, R., and Schwarcz, H.P., 2004, Constraints on Pleistocene pluvial climates through stable-isotope analysis of fossil-spring tufas and associated gastropods, Kharga Oasis, Egypt: Palaeogeography, Palaeoclimatology, Palaeoecology, v. 206, p. 157–175, doi: 10.1016/j.palaeo.2004.01.021.

Spotl, C., and Vennemann, T.W., 2003, Continuous-flow isotope ratio mass spectrometric analysis of carbonate minerals: Rapid Communications in Mass Spectrometry, v. 17, p. 1004–1006.

Sun, H., Liu, Z., and Yan, H., 2014, Oxygen isotope fractionation in travertine-depositing pools at Baishuitai, Yunnan, SW China: Effects of deposition rates: Geochimica et Cosmochimica Acta, v. 133, p. 340–350, doi: 10.1016/j.gca.2014.03.006.

Szabo, B.J., 1990, Ages of travertine deposits in eastern Grand Canyon National Park, Arizona: Quaternary Research, v. 34, p. 24–32.

Tafoya, A.J., 2012, Uranium-series geochronology and stable isotope analysis of travertine from Soda Dam, New Mexico: A Quaternary record of episodic spring discharge and river incision in the Jemez Mountains hydrothermal system [M.S. thesis]: Albuquerque, University of New Mexico, 104 p.

Turi, B., 1986, Stable isotope geochemistry of travertines, *in* Fritz, B.P. and Fontes, J.C. eds., Environmental Isotope Geochemistry: Amsterdam, Elsevier, p. 207–235.

Uysal, I.T., Feng, Y., Zhao, J. -x., Altunel, E., Weatherley, D., Karabacak, V., Cengiz, O., Golding, S.D., Lawrence, M.G., and Collerson, K.D., 2007, U-series dating and geochemical tracing of late Quaternary travertine in co-seismic fissures: Earth and Planetary Science Letters, v. 257, p. 450–462, doi: 10.1016/j.epsl.2007.03.004.

Vylita, T., Zak, K., Cilex, V., Hercman, H., and Miksikova, L., 2007, Evolution of hot-spring travertine accumulation in Karlovy Vary/Carlsbad (Czech Republic) and its significance for the evolution of Tepla valley and Ohre/Eger rift: Zeitschrift Fur Geomorphologie, v. 51, p. 427–442, doi: Doi 10.1127/0372-8854/2007/0051-0427.

Wang, H., Yan, H., and Liu, Z., 2014, Contrasts in variations of the carbon and oxygen isotopic composition of travertines formed in pools and a ramp stream at Huanglong Ravine, China: Implications for paleoclimatic interpretations: Geochimica et Cosmochimica Acta, v. 125, p. 34–48, doi: 10.1016/j.gca.2013.10.001.

Williams, A.J., Crossey, L.J., Karlstrom, K.E., Newell, D., Person, M., and Woolsey, E., 2013, Hydrogeochemistry of the Middle Rio Grande aquifer system — Fluid mixing and salinization of the Rio Grande due to fault inputs: Chemical Geology, v. 351, p. 281–298, doi: 10.1016/j.chemgeo.2013.05.029.

Yan, H., Sun, H., and Liu, Z., 2012, Equilibrium vs. kinetic fractionation of oxygen isotopes in two low-temperature travertine-depositing systems with differing hydrodynamic conditions at Baishuitai, Yunnan, SW China: Geochimica et Cosmochimica Acta, v. 95, p. 63–78, doi: 10.1016/j.gca.2012.07.024.

*Supplemental data can be found at http://nmgs.nmt.edu/repository/index.cfml?rid=2016004*